Article

Not peer-reviewed version

The Synergy Between Methanol M100 and Plasma Assisted Ignition System PAI to Achieve Increasingly Leaner Mixtures in a Single-Cylinder Engine.

Federico Ricci , Francesco Mariani , Stefano Papi , Jacopo Zembi * , Michele Battistoni , Carlo Nazareno Grimaldi

Posted Date: 5 March 2024

doi: 10.20944/preprints202403.0226.v1

Keywords: lean combustion; kinetic; methanol fuel; Plasma Assisted Ignition; SI engine

Article

The Synergy between Methanol M100 and Plasma Assisted Ignition System PAI to Achieve Increasingly Leaner Mixtures in a Single-Cylinder Engine

Federico Ricci [1], Francesco Mariani [1], Stefano Papi [2], Jacopo Zembi [1,*], Michele Battistoni [1] and Carlo Nazareno Grimaldi [1]

[1] University of Perugia, Department of Engineering, Via G. Duranti 93 06125 Perugia (PG) - Italy
[2] Federal-Mogul Powertrain Italy, Via della Scienza, 6/8, 41012 Carpi (MO) - Italy
* Correspondence: jacopo.zembi@unipg.it

Abstract: Currently, conventional spark-ignition engines face challenges in meeting the ever-growing demands of customers and increasingly stringent regulations regarding pollutant emissions. A combination of innovative strategies and carbon-neutral fuels is deemed necessary in order to further reduce fuel consumption and minimize engine emissions. The present work aims to assess the performance of combustion strategies using low-carbon content fuel, such as methanol M100, ignited by a plasma-assisted igniter (PAI) under ultra-lean conditions. The experimental campaign is conducted on a single-cylinder research engine at different engine speeds and low loads, moving up to the engine lean stable limits. To determine the benefits brought by the proposed strategy, referred to as M100-PAI, the obtained outcomes are compared with the ones obtained using market gasoline E5 ignited by the PAI system and conventional spark. The synergy between M100 (methanol) and Plasma Assisted Ignition (PAI) in internal combustion engines yielded notable benefits. This combination significantly improved combustion stability if compared to the other combinations tested, by extending the lean stable limit to λ=2.0, reducing cycle-to-cycle variability, and facilitating faster flame front acceleration, resulting in enhanced homogeneity. These enhancements, obtained with the combination M100-PAI, contributed to higher fuel efficiency showing a 10% efficiency gain over the combination E5-gasoline spark ignition.

Keywords: lean combustion; kinetic; methanol fuel; Plasma Assisted Ignition; SI engine

1. Introduction

The increasingly stringent regulations on emissions of harmful gases: NOx, CO, Uhc, soot, and CO_2 have forced the entire engine research community to improve the thermal efficiency and emission characteristics of spark-ignition (SI) engines [1]. Advanced combustion techniques such as cooled external exhaust gas recirculation (EGR) [2], engine boosting in conjunction with downsizing [3], water injection [4,5] and lean mixture operations [6] proved to be effective ways to meet these demands. Due to the carbon content of commercial fossil fuels, it is difficult for even the most efficient systems with low emissions to achieve zero CO_2 content [7]. Therefore, the integration of innovative and carbon-neutral strategies is deemed necessary to achieve net zero emissions targets [8]. The scientific community is currently investigating renewable energy sources (electro-fuels also known as e-fuels [8,10]) and fuels deriving from waste biomass (biofuels [11]) for their low *cradle-to-grave* carbon impact [12]. Among the others, pure methanol M100 is the simplest liquid synthetic fuel and one of the most promising alternative fuels for replacing petroleum-based fuels [13]. Methanol has the potential to burn easily in the air due to its high volatility [14]. Methanol has a higher Research Octane Number (RON) and a heat of vaporization greater than gasoline [15]. A high heat of vaporization cools down the incoming charge, thus improving volumetric efficiency and power output. A higher RON can increase thermal efficiency as it can increase the compression ratio. This feature renders M100 suitable for small, turbocharged, high-power-density engines [16]. Furthermore, as a liquid fuel, M100 has the advantage over gasoline because its initial boiling point

 doi:10.20944/preprints202403.0226.v1

makes it safely stored and distributable with existing infrastructures [17]. In the literature, it has been reported that the use of methanol as an alternative fuel in internal combustion engines has achieved excellent results in terms of engine performance and emissions. Celik et al. [17] studied the effect of increasing the compression ratio of a single-cylinder engine fueled with M100. They found enhancement in engine power and BTE (Brake Thermal Efficiency) of about 14% and 36%, respectively, moving from 6:1 to 10:1. Moreover, CO, CO_2, and NOx emissions were reduced by about 37%, 30% and 22%, respectively. The methanol combustion process and the presence of a single carbon molecule (CH_3OH) reduce NOx and PM emissions compared to complex hydrocarbon fuels [18]. Dhaliwal et al. [19] found that using pure methanol instead of compressed natural gas (CNG), liquified petroleum gas (LPG) and M85, drastically decreases the emissions of NOx and PM of both light and heavy-duty vehicles. The higher oxygen content in methanol faster the flame and the lower the CO and HC emissions [20]. However, at ultra-lean mixture conditions, towards which the research is directed, the lower energy density (LHV_{M100} = 19,93 MJ/kg) and the higher heat of vaporization (HoV_{M100} = 1160 kJ/kg at 25°C) of methanol compared to gasoline (LHV_{E5} = 44 MJ/kg and HoV_{E5} ~ 380 kJ/kg at 25°C) reduces the mixture ignition capabilities causing slow-burning thermodynamic cycles featured with high variability and partial oxidation products as HC and CO. High ignition energies are consequently deemed necessary under extreme operating conditions to address these issues. Traditional spark-based solutions are inefficient in transferring energy to the gas under challenging conditions [21,22]. Abidin and Chadwell [23] estimated that only 2.5% of the primary energy reaches the medium. Solutions such as multiple spark discharge [24] and high-energy discharge [25] improve ignition effectiveness and combustion stability but share limitations with traditional spark plugs, including small plasma volume, electrode heat losses, erosion, and fouling [26]. Advanced ignition concepts aim to enhance discharge energy, efficiency, and volume. Plasma-jet ignition systems [27] and pre-chamber ignition systems [28] enable lean/dilute conditions but involve design complexities and combustion chamber adaptation. In recent years, extensive research has focused on plasma-assisted ignition systems (PAI) [29], also known as low-temperature plasma (LTP) ignition systems. PAI ensures stable combustion under critical conditions by generating non-equilibrium plasma with a significant temperature difference between electrons (hot) and heavy species (cold) in the gas [30]. This volumetric discharge mode, combined with kinetic, transport, and thermal effects, reduces ignition delay, accelerates kernel formation, and its evolution [31]. Electron impact produces excited species and active radicals like hydroxyl radicals OH*, O, O_3, reducing fuel oxidation reaction time [**Error! Reference source not found.**,32]. Collisions between discharged particles and gas molecules increase turbulence and mixing, while the thermal effect promotes fuel oxidation and accelerates combustion initiation according to Arrhenius law [34].

1.1. Present Contribution

The present work evaluates the possibility to exploit the above-mentioned benefits of M100 at ultra-lean conditions by using a high-energy PAI, namely a Barrier Discharge Igniter (BDI) [35,36]. Several studies [6,37,38] have demonstrated the capability of BDI to promote stable combustion processes in conditions of lean mixtures. This is made possible by creating non-equilibrium plasma (or LTP), which uses the combined action of the three abovementioned effects to hasten the development of early flames [39,40]. Therefore, by harnessing the inherent advantages of M100, BDI and lean blends, this work reports the outcomes of a combustion strategy able to address the challenge of reducing consumption. The test campaign was performed at fixed load and 1000 rpm in a single-cylinder research engine by performing indicating analysis. Comparisons between market gasoline E5 ignited by BDI and traditional spark were realized to estimate the advantages brought by the proposed strategy in terms of engine management, combustion behavior, and ability to extend the engine's lean stable limit. The results show that, the combination of methanol with PAI in ICE offers a compelling array of advantages. This pairing substantially enhances combustion stability by extending the lean stable limit to λ=2.0. It fosters faster flame front acceleration during the initial combustion phase, leading to reduced cycle-to-cycle variability and greater homogeneity within the air-fuel mixture. These improvements result in higher fuel efficiency, with M100-PAI achieving a

 doi:10.20944/preprints202403.0226.v1

remarkable 10% efficiency gain compared to conventional spark ignition with E5. Furthermore, the improved combustion stability under lean conditions provides the potential for reduced emissions of unburned hydrocarbons and carbon monoxide. The smoother rise in CoV_{IMEP}, when λ values become leaner, indicates enhanced stability and robustness in challenging operating conditions. This combination capitalizes on methanol's inherent properties, such as its oxygen-rich composition and rapid burning rate, which contribute to a broader flammability range and more consistent combustion. As a result, M100-PAI demonstrates promise not only in improving engine efficiency but also in achieving a higher level of homogeneity within the combustion chamber.

2. Materials and Methods

A 500-cc single-cylinder research engine is used to perform the test campaign (Table 1). The engine has four valves, a reverse tumble intake port system and a pent-roof combustion chamber with the igniter centrally located. Conventional mineral lubricant at 343.0 ± 0.2 K is used for all the other moving parts of the engine to guarantee engine durability and reduced blow-by [41]. Methanol M100 and gasoline E5 are injected in the intake port by a Weber IWP092 port fuel injector at 4.8 bar absolute (Table 2). The air-fuel ratio (λ) is modified by varying the fuel amount at fixed throttle position (i.e., 10%, idle mode). A Kistler Kibox combustion analysis system is used to perform indicating analysis, with a temporal resolution of 0.1 CAD. At each operating point tested, 100 consecutive events are recorded. The innovative igniter employed in this work, i.e., the Barrier Discharge Igniter (BDI) [42,43], is controlled by a dedicated power electronic system (ACIS Box) at 1.04 MHz and its discharge control parameters, i.e., activation time ton and the driving voltage V_d are managed by a dedicated software [45,46]. The first control parameter, i.e., t_{on}, defines the discharge duration while the second one, i.e., V_d, is proportional to the electrode voltage occurring on the igniter firing end and regulates the development of ionization waves, i.e., streamers, around the igniter's dielectric alumina globe [36]. The firing end contains the counter electrode and it prevents the streamer-to-arc transition phenomenon which causes the loss of all benefits brought by the non-thermal plasma discharge [47–52] (Figure 1).

Table 1. Engine data [46].

Displaced volume	500 cc
Stroke	88 mm
Bore	85 mm
Connecting Rod	139 mm
Compression ratio	8.8:1
Number of Valves	4
Exhaust Valve Open	13 CAD bBDC
Exhaust Valve Close	25 CAD aTDC
Inlet Valve Open	20 CAD bTDC
Intake Valve Close	24 CAD aBDC

Table 2. Physical properties of the used fuels.

Properties	Gasoline (E5)	Methanol (M100)
C/H ratio [-]	0.54	0.25
O/C ratio [-]	0.03	1
Density [kg/m^3]	761.42	792
Lower heating value [MJ/kg]	44	19.93
Heat of vaporization [kJ/kg]	349	1160
Stoichiometric air-to-fuel ratio	14.7	6.4
Research octane number (RON)	95-98	109
Autoignition temperature [K]	536-853	738

Preprints.org (www.preprints.org) | NOT PEER-REVIEWED | Posted: 5 March 2024 doi:10.20944/preprints202403.0226.v1

Adiabatic Flame Temperature [°C]	2002	1870
Laminar flame speed at the normal temperature and pressure, $\lambda = 1$ (cm/s)	28	42
Flammability limit in air (λ)	0.26–1.60	0.23–1.81

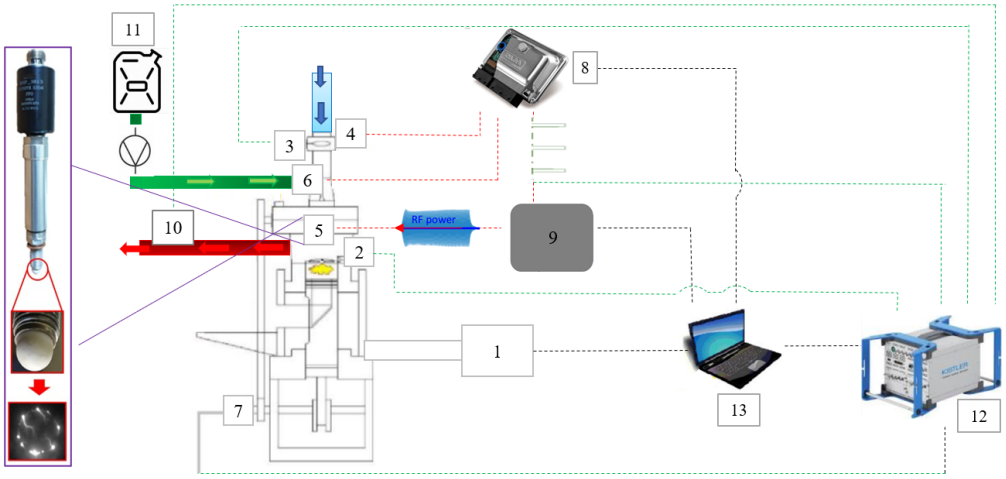

1 - AVL 5700 dynamic brake for engine control both in motored and firing conditions
2 - Kistler 6061 B piezoelectric transducer for in-cylinder pressure
3 - Kistler 4075A5 piezoresistive transducer for intake pressure
4 – throttle valve opening controller
5 – Advanced Corona Ignition System
6 – injector
7 - AVL 365C optical encoder for absolute crank angular position
8 – Athena GET HPUH4 Engine Control Unit
9 – ACIS box. Electronic system high-frequency amplifier
10 – λ-NOx sensor
11 – Fuel tank and pump
12 – Kistler Kibox combustion analysis system
13 – control interface for ACIS, ECU, KIBOX and dynamic brake

Figure 1. Representation of the experimental setup with a focus on the PAI system and corresponding development of the streamers around its firing end.

3. Case Study

In the first part of the work, the test campaign was carried out with the engine operating in idle mode at 1000 rpm, from λ=1.2 up to the lean stable limit found for each analyzed case. The performance of the proposed strategy, i.e., M100 and BDI, was compared with the ones resulting from the usage of BDI-E5, spark-M100 and spark-E5. Tests were carried out by taking as a reference baseline the latter configuration. For each λ value, the ignition timing of spark-E5 was set to obtain the maximum brake torque (MBT), which can be detected with the in-cylinder peak pressure (AP_{max}) in a range of 11-17 CAD (Figure 2a). As shown in Figure 2b, using the same ignition timing (IT) with a fixed λ value ensured that all combinations fell within the MBT range. This made it easier to compare how flames formed and developed in these combinations, as they all began from the same in-cylinder conditions. Moving to ultra-lean points, the IT selection was changed to the BDI-M100 test case due to combustion stability reasons.

The control parameters of BDI were set at V_d = 60V, t_{on} = 1500µs [37]. For the spark system, only the ignition coil dwell time can be managed, and it was set to 3.1 ms for all tested points. Table 3 resumes all the operating points evaluated in this work.

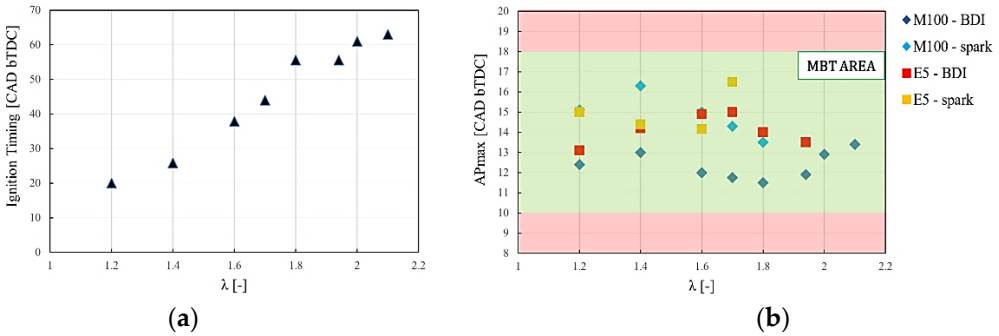

(a) (b)

 doi:10.20944/preprints202403.0226.v1

Figure 2. Ignition timings (a) for each tested lambda and corresponding angular position of the in-cylinder peak pressure (b). Moving to ultra-lean points, the IT selection was changed to the BDI-M100 test case due to combustion stability reasons. For such a reason, for reason, up to 1.9 only the combination BDI-M100 shows AP_{max} values.

Table 3. Operating point tested.

λ	1.2	1.4	1.6	1.7	1.8	1.9	2.0	2.1
Combination Igniter-Fuel	BDI-M100 BDI-E5 SPARK-M100 SPARK-E5	BDI-M100 BDI-E5 SPARK-M100 SPARK-E5	BDI-M100 BDI-E5 SPARK-M100 SPARK-E5	BDI-M100 BDI-E5 SPARK-M100	BDI-M100 BDI-E5 SPARK-M100	BDI-M100 BDI-E5	BDI-M100	BDI-M100

4. Results and Discussions

4.1. Combustion Stability

Coefficient of Variance (CoV) of the Indicated Mean Effective Pressure (IMEP), i.e., the ratio between IMEP standard deviation and IMEP mean value, is used to evaluate the combustion stability. Each operating point is considered stable if the CoV_{IMEP}<4%.

Figure 3 displays the CoV_{IMEP} (Equation (1)), values for each combination from λ=1.2 up to the corresponding lean stable limit with the engine operating at 1000 rpm.

$$CoV_{IMEP} = \frac{\sigma_{IMEP}}{\mu_{IMEP}} x\ 100 = \frac{std\ deviation\ in\ IMEP}{mean\ IMEP}\ x\ 100 \quad (1)$$

The combinations are stable, with no remarkable differences, up to λ=1.6. As the mixture becomes leaner, the probability of ignition decreases due to the absence of available fuel and the decrease in temperature caused by excess air [53]. This leads to an increase in cycle-to-cycle variability [37]. In the richest cases, the availability of fuel to be ignited does not highlight differences between the tested combinations in terms of stability [38].

Starting from the spark results, at λ=1.7, E5-spark becomes unstable whereas the combinations M100-spark operating with oxygenated fuels maintains stable processes up to such λ. The presence of oxygen in the fuel is crucial in keeping the CoV_{IMEP} below the stability threshold of 4%. The findings of [54], which showed a comparison between M100 and E5 performance on a 4-cylinder PFI SI engine under idle conditions and low speed under diverse air-fuel ratios (λ), can elucidate such a behavior. M100's higher diffusion rate and elevated oxygen content lead to enhanced uniformity in the air-fuel mixture, resulting in reduced CoV within the intake port compared to gasoline. The greater Heat of Vaporization (HoV) inherent to M100, which might normally hinder the evaporation process, is counterbalanced by the engine's low speed. Despite M100's lower LHV, its combustion stability prevails over gasoline due to faster flame propagation facilitated by the heightened homogeneity and oxygen content. Notably, minimizing the initial part of combustion process is an effective method for enhancing combustion stability [52]. Furthermore, in contrast to gasoline's sharp increase in CoV_{IMEP} with leaner mixtures (higher λ), methanol exhibits a smoother rise, attributed to its accelerated burning rate and broader flammability range, which enhance stability under lean conditions.

Approaching leaner conditions, at λ=1.8 all the combinations using the spark-plug igniter fail to guarantee CoV_{IMEP} below the stability threshold, whereas BDI enables repeatable combustion processes. This finding implies the effect of BDI discharge on combustion robustness and repeatability [36,38]. BDI extends the lean stable limit of E5-spark of 0.2 λ units, i.e., up to λ = 1.8. BDI

 doi:10.20944/preprints202403.0226.v1

is dedicated to the production of high number of chemical species, especially ozone O_3, by involving considerable volume mixture around its firing-end [55]. O_3 results in its decomposition into monatomic oxygen which allows a faster oxidation of the fuels thus accelerating the chain-branching reactions and consequently increase the burning velocity [56]. It has been observed [45] that when operating under conditions close to stoichiometry, BDI's oxygen impact is most pronounced during the initial combustion phase. However, as the mixture becomes leaner, the kinetic effect appears to diminish. This behavior indicates that the primary influence is thermal, while the presence of radicals plays a secondary role, particularly under lean conditions with advanced ignition timing. These findings suggest that BDI primarily extends the stable operating limit through its high amount of energy release into the medium compared to spark [42,43], in conjunction with the volumetric characteristics of its discharge which can involve a larger portion of the combustion chamber with respect to traditional thermal ignition [37]. However, when operating with methanol, BDI is capable of extends the engine stable limit to be extended up to λ=2.0, resulting in 0.2 λ units gain over the E5-BDI and in 0.3 λ units gain over the M100-spark. Therefore, the difference between the λ gain between BDI-M100 and M100-spark is 0.1 λ higher than the gain between E5-BDI and E5-spark. This outcome could suggest that the oxygen presence aids in the production of active and radical species as a result of the non-equilibrium plasma discharge interaction with M100, thereby improving kernel formation mechanisms and robustness. Masurier and colleagues [56] demonstrated that the addition of O_3 (a byproduct of a BDI discharge), to methanol fuel accelerates flame front evolution. As previously reported, this acceleration allows to extend the lean stable limit of the engine and could provide an explanation for the higher λ extension when BDI-M100 is employed.

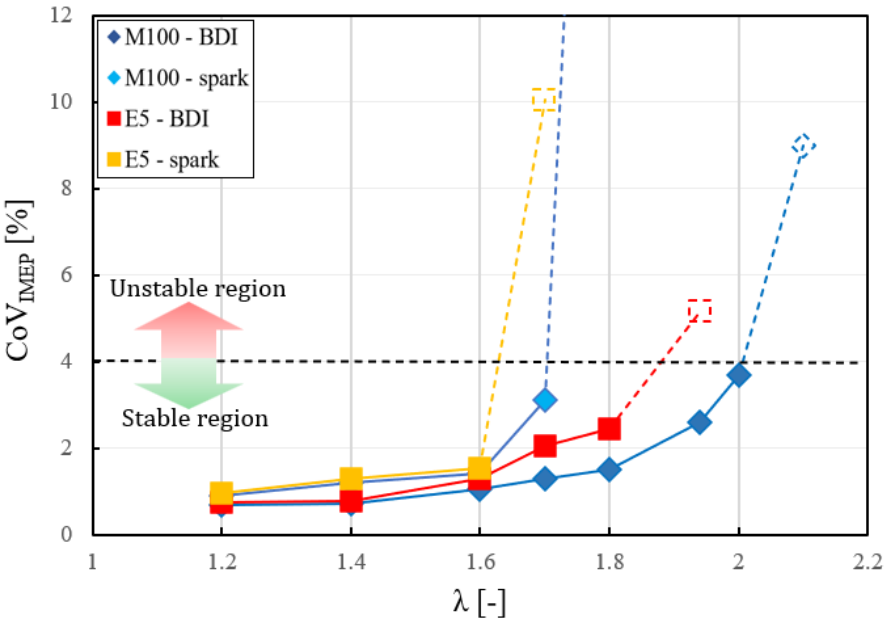

Figure 3. CoV_{IMEP} plotted against λ at 1000 rpm. For the sake of clarity, operating points showing CoV_{IMEP} > 4 % are indicated through dotted markers.

4.2. Combustion Duration

To emphasize these findings, Figure 4a provides insights into the duration of the first part of the combustion process, i.e., CA0-10 which represents the time required by the combustion process to burn 10% of the entire mass. For comparison purposes, the operating points up to the limit found with spark-E5 (λ=1.6) have been considered. As increasingly leaner mixtures are used, the CA0-10 increases due to the lower fuel content, resulting in a lower average in-cylinder temperature [38]. From the graph, it is possible to highlight the findings as previously stated. Considering the same fuel, BDI is capable of accelerating the flame front. This outcome proves again the capability of PAI discharge to enhance the rate of burning through thermal effect and by exploiting the early

 doi:10.20944/preprints202403.0226.v1

production of active chemical species combined with a larger volume of mixture involved by the discharge [37]. When using the same ignition system, methanol accelerates the flame front. When an oxygenated fuel is used, the larger disposal of oxygen within the mixture together with the higher homogeneity compared to E5, promotes chemical oxidation thus reducing the duration of the chain reaction mechanism [39]. The combination of BDI-M100, leveraging the benefits of the PAI discharge and those observed with methanol, produces the fastest acceleration of the flame front. Faster initial combustion corresponds to processes characterized by lower cycle-to-cycle variability. At each compared λ, the lower the CA0-10 the lower the CoV_{IMEP} (over-imposed in grey on the bars of Figure 4a). With M100, it is possible to observe a slower drop in cycle-to-cycle variation, which is even less pronounced when this fuel is ignited by a PAI discharge (refer to the trend line of the curves in Figure 4b).

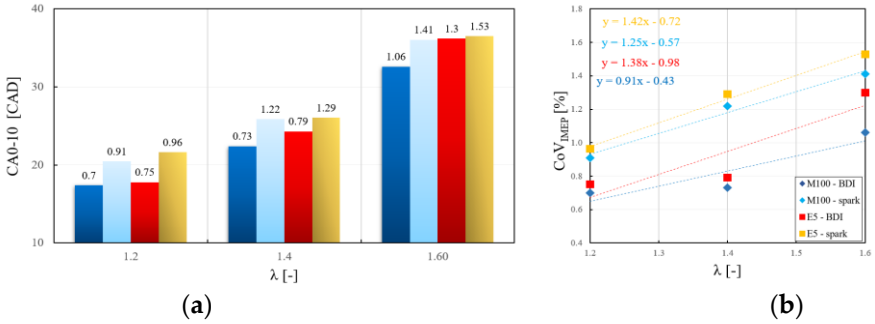

Figure 4. (a) Crank angle combustion duration from ignition timing to 10% MFB (Mass Fraction Burned) for all tested combination of igniter/fuel up to 1.6. Overimposed, in grey, the CoV_{IMEP} value of each operating point. (b) Focus on the first three point tested with the corresponding linear trend and equation to emphasize the rise of CoV_{IMEP} of each combination.

Figure 5 provides insights into the entire combustion process CA10-90. To explain the combustion behavior in such a stage, in Figure 5 beside the CA10-90 is reported the trend of the maximum in-cylinder pressure (P_{max}) and again the CA0-10. In general terms, the CA10-90 exhibits an opposite trend compared to the CA0-10. This trend is consistent for both analyzed fuels and may be somewhat challenging to explain. However, it could be related to the timing of combustion and the somewhat unconventional behavior of blow-by in the optical research engine due to the use of non-standard piston rings [38]. The hypothesis is that if the initial phase of combustion happens more rapidly, it can result in a higher rate of pressure increase and absolute pressure in the entire combustion chamber, including the unburned gas area. This, in turn, could lead to more unburned air-fuel mixture escaping through gaps, avoiding the advancing flame, and consequently slowing down the second phase of combustion. Apart from singularities, BDI-M100 and BDI-E5 show fastest CA0-10 (Figure 5a) which gain the maximum in-cylinder pressure at higher level if compared to the other two spark combinations (Figure 5b). This leads, in general, to slowest CA10-90 in all the three λ cases analyzed. To make an example, at λ=1.4 BDI shows CA0-10 = 22.4 CAD and CA0-10 = 24.3 CAD with M100 and E5, respectively, whereas spark presents CA0-10 equals to 25.89 and 26.07 CAD when ignites methanol and gasoline. Therefore, BDI gains on average the spark P_{max} of about 7%. As a consequence of this, spark shows the fastest CA10-90 with both fuels. It is worth highlighting that, despite the similar level of P_{max} between spark-M100 and spark-E5, the faster CA10-90 showed by gasoline could be related to the higher presence of hydrocarbon which speeds up the flame in the part final combustion.

Preprints.org (www.preprints.org) | NOT PEER-REVIEWED | Posted: 5 March 2024 doi:10.20944/preprints202403.0226.v1

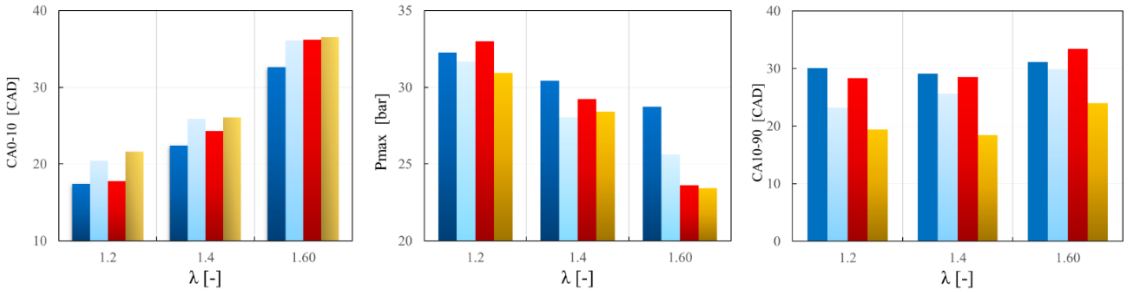

Figure 5. (a) Crank angle combustion duration from ignition timing to 10% MFB for all tested combination of igniter/fuel up to 1.6. (b) Trend of the maximum in-cylinder pressure for the same lambda values, (c) and Crank angle combustion duration from 10% of MFB to 90%.

4.3. Indicated Work and Efficiency

The indicated fuel conversion efficiency is computed by considering the indicated work per cycle $\mathcal{L}_{ind}$, the fuel's lower heating value LHV, and the injected fuel mass per cycle m_f (Equation (2)).

$$\eta_{ind} = \frac{\mathcal{L}_{ind}}{m_f \cdot LHV} \tag{2}$$

The latter quantities m_f is determined by considering the injector's mass flow rate curves and injection timing. At the same λ value, all the combinations present similar $\mathcal{L}_{ind}$ (Figure 6a) since positioned within the MBT range (see Figure 2b). The indicated work decreases as λ increases due to lower amount of mixture to be ignited [51]. The higher the capability of the tested combinations to extend the lean stable limit the less pronounced the reduction on the delivered work. Figure 6b reports the trend of η_{ind} at each stable lambda analyzed for the different igniter-fuel combinations.

Methanol provides the highest indicated thermal efficiency regardless of the igniter used. For example, at λ= 1.2, M100 guarantees improvements of about 12% over E5. As a result, these findings contribute to the reduction of CO_2 emissions when methanol is employed instead of gasoline [38]. The higher efficiency of M100 can be associated to the additional oxygen content which fosters combustion initiations and allows for more complete events. Methanol helps enhance emissions performance for hydrocarbons (HC) and carbon monoxide (CO) during idle lean burn conditions by promoting better uniformity in the air-fuel mixture [54]. When considering the same fuel (e.g.,: E5-BDI, E5-spark), BDI exhibits higher efficiencies. Going towards leaner mixtures BDI achieves higher η_{ind} presenting, at the same time, marked instability with regards to spark and stable processes, instead, when the PAI discharge is employed. When BDI-M100 is employed, the combined effect of PAI discharge together with the higher oxygen content allows to improve on average: η_{ind} of about 10%, 9% and 2.5%, over spark-E5, BDI-E5, and spark-M100, respectively.

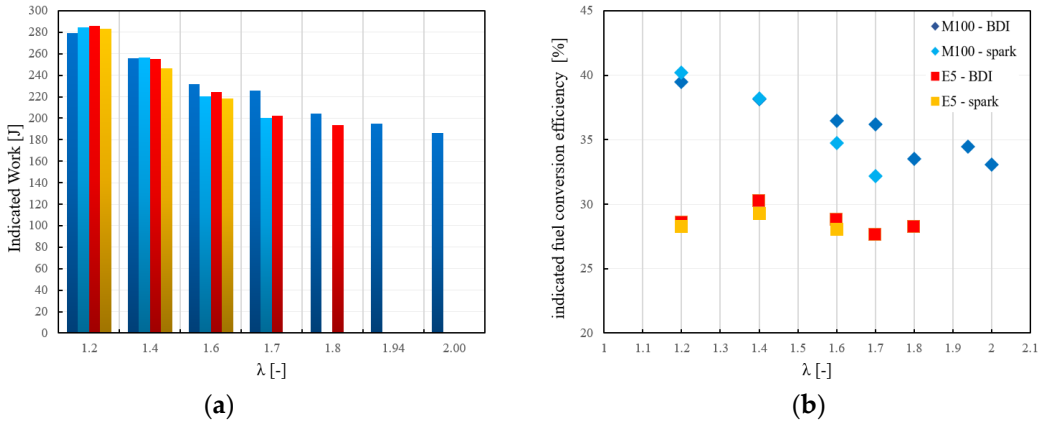

Figure 6. (a) Indicated work and (b) corresponding fuel conversion efficiency against λ for each tested combination.

 doi:10.20944/preprints202403.0226.v1

4.4. Nitrogen Oxides Emissions

Figure 7 displays a graph where nitrogen oxides emissions are plotted against λ for different igniter/fuel combinations. To make the data easier to visualize, the emissions values have been scaled relative to the highest recorded value (1 on the graph corresponds to approximately 4500 ppm). The emission of NOx from both gasoline and methanol combinations significantly decreased as the excess air coefficient increased, primarily because this led to a reduction in the combustion temperature [37].

When spark is employed, the use of methanol resulted in a lower combustion temperature due to its lower adiabatic flame temperature [54]. This mitigates the effect on the formation of NOx compared to using gasoline.

BDI enhances the NOx production in the lowest λ range, especially when M100. The BDI-E5 combination presents a higher level of emissions compared to spark-E5 due to the local deposition of monoatomic oxygen which can react to NOx. In the BDI-M100 case, when oxygen is sourced not just from the air but also from the fuel itself, its presence both at and behind the flame front undergoes alterations [38]. This led to augmented production of NOx emissions. From another point of view, such results highlight that operating with the combination M100 - PAI, the greater presence of oxygen, extends the lean stable limit (Figure 3) and the NOx emission trend (Figure 7).

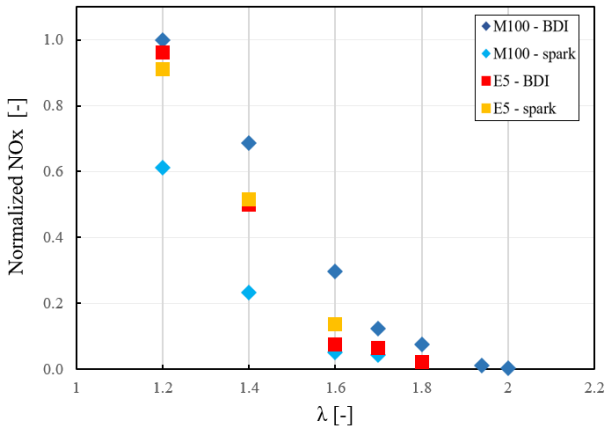

Figure 7. Normalized NOx trend from λ=1.2 up to the lean stable limit found for each tested combination.

5. Conclusions

By harnessing the inherent advantages of pure methanol (M100), innovative ignition systems such as BDI, and lean blends, the present work evaluated the results of a combustion strategy capable of addressing the challenge of reducing fuel consumption and emission of internal combustion engines. The test campaign was conducted in a single-cylinder research engine at fixed load moving from a slightly lean case to the lean stable limit and at different speed conditions. Comparisons between market gasoline E5 ignited by BDI and traditional spark were performed to estimate the advantages brought by the proposed strategy. At fixed engine speed (1000 rpm) the comparison between M100 and E5 ignited by a traditional spark and BDI showed that:

Combustion Stability:

CoV_{IMEP} was used to evaluate combustion stability, with a stability threshold set at 4%. Up to a lean mixture (λ) of 1.6, all combinations showed a stable combustion. Oxygenated fuels, like M100, exhibited better stability due to their higher oxygen content, leading to enhanced uniformity in the air-fuel mixture. The use of a Plasma Assisted Ignition as BDI system extended the lean stable limit significantly, especially when paired with methanol (up to λ = 2.0), demonstrating the effectiveness of BDI in improving combustion stability.

Combustion Duration:

 doi:10.20944/preprints202403.0226.v1

The duration of the initial combustion phase (CA0-10) increased with leaner mixtures, reflecting the lower fuel content and reduced in-cylinder temperature. BDI and methanol accelerated the flame front, resulting in faster initial combustion and lower cycle-to-cycle variability.

Indicated Work and Efficiency:

Indicated fuel conversion efficiency was computed with all combinations showing similar indicated work within the MBT range. Methanol consistently provided the highest thermal efficiency, contributing to reduced CO_2 emissions compared to gasoline.

BDI improved efficiency by extending the lean stable limit and promoting stable processes. Finally, the combination BDI-M100 showed the highest efficiency gains, attributed to the combined effects of PAI discharge and oxygen content.

Nitrogen Oxides Emissions (NOx):

NOx emissions decreased as excess air (λ) increased, primarily due to reduced combustion temperatures. Methanol resulted in lower NOx emissions compared to gasoline when spark ignition was used. BDI enhanced NOx production at lower λ values, especially with M100, due to increased oxygen availability from the fuel and altered oxygen dynamics. However, the ability to PAI-M100 to extend the lean stable limit can lead close to zero emissions of NOx (see Figure 7 for λ=2).

Future research should aim to optimize this combination for both efficiency and emissions control, enabling its potential for reducing greenhouse gas emissions in practical applications.

Author Contributions: Conceptualization, F.R. and F.M.; methodology, F.R.; software, F.R.; validation, F.R. and F.M.; formal analysis, F.R.; investigation, F.R. and F.M.; resources, C.N.G. and S.P..; data curation, F.R..; writing-original draft preparation, F.R.; writing-review and editing, J.Z., M.B., C.N.G. and S.P..; visualization, F.R.; supervision, J.Z., M.B., and C.N.G..; project administration, C.N.G.; funding acquisition, C.N.G. All authors read and agreed to the published version of the manuscript.

Funding: The research has been partially funded by the University of Perugia grant "Fondo Ricerca di Ateneo, edizione 2021". The igniters used for the research have been provided by Federal Mogul Powertrain Italy, a Tenneco Group Company.

Data Availability Statement: Dataset available on request from the authors.

Conflicts of Interest: The authors declare no conflict of interest.

Nomenclature

ACIS	Advanced Corona Ignition System
AP_{max}	crank angle degree at the maximum in-cylinder pressure
aTDC	after the top dead center
BDI	barrier discharge igniter
CAD	crank angle degree
CoV	coefficient of variation
E5	European market gasoline
ECU	engine control unit
EGR	Exhaust Gas Recirculation
ICE	internal combustion engine
IMEP	indicated mean effective pressure
LTP	Low-Temperature Plasma
M100	methanol
MBT	maximum brake torque
MON	motor octane number
PFI	port fuel injection

 doi:10.20944/preprints202403.0226.v1

RF	radio-frequency
SI	spark ignition
t_{on}	corona activation time
V_d	driving voltage
λ	relative air-fuel ratio

References

1. Reitz RD, Ogawa H, Payri R,. IJER editorial: the future of the internal combustion engine. Int J Engine Res 2020;21:3–10. Doi: 10.1177/1468087419877990
2. Xiumin Yu, "Experimental study on the effects of EGR on combustion and emission of an SI engine with gasoline port injection plus ethanol direct injection", Fuel, Volume 305, 2021, 121421, ISSN 0016-2361, Doi: 10.1016/j.fuel.2021.121421
3. Zsiga, N.; Voser, C.; Onder, C.; Guzzella, L. Intake Manifold Boosting of Turbocharged Spark-Ignited Engines. Energies 2013, 6, 1746–1763, Doi:10.3390/en6031746
4. J. Zembi, et al. "Numerical investigation of water injection effects on flame wrinkling and combustion development in a GDI spark ignition optical engine." SAE Technical Paper, 2021, 2021-01-0465. Doi: 10.4271/2021-01-0465
5. J. Zembi, et al. "Investigations on the impact of port water injection on soot formation in a DISI engine through CFD simulations and optical methods." Fuel, 2023, 337, 127170. Doi: 10.1016/j.fuel.2022.127170
6. Ricci, F., Petrucci, L., Cruccolini, V., Discepoli, G., Grimaldi, C. N., & Papi, S. (2020). Investigation of the Lean Stable Limit of a Barrier Discharge Igniter and of a Streamer-Type Corona Igniter at Different Engine Loads in a Single-Cylinder Research Engine. Proceedings, 58(1), 11. Doi: 10.3390/wef-06909
7. James P. Szybist, What fuel properties enable higher thermal efficiency in spark-ignited engines? Progress in Energy and Combustion Science, Volume 82, 2021, 100876, ISSN 03601285, Doi: 10.1016/j.pecs.2020.100876
8. F. Ausfelder and K. Wagemann, "Power-to-Fuels: E-Fuels as an Important Option for a Climate-Friendly Mobility of the Future," Chemie-Ingenieur-Technik, vol. 92, no. 1–2, pp. 21–30, 2020. Doi: 10.1002/cite.201900180
9. L. E. Hombach, L. Doré, K. Heidgen, H. Maas, T. J. Wallington, and G. Walther, "Economic and environmental assessment of current (2015) and future (2030) use of E-fuels in light-duty vehicles in Germany," J. Clean. Prod., vol. 207, pp. 153–162, 2019. Doi: 10.1016/j.jclepro.2018.09.261
10. Ballal, Vedant. "Climate change impacts of e-fuels for aviation in Europe under present-day conditions and future policy scenarios." Fuel 338 (2023): 127316. Doi: 10.1016/j.fuel.2022.127316
11. Puricelli, G. Cardellini, S. Casadei, D. Faedo, A. E. M. van den Oever, and M. Grosso, "A review on biofuels for light-duty vehicles in Europe," Renew. Sustain. Energy Rev., vol. 137, no. November 2019, p. 110398, 2021. Doi: 10.1016/j.rser.2020.110398
12. A. I. Osman, N. Mehta, A. M. Elgarahy, A. Al-Hinai, A. H. Al-Muhtaseb, and D. W. Rooney, Conversion of biomass to biofuels and life cycle assessment: a review, vol. 19, no. 6. Springer International Publishing, 2021. Doi: 10.1007/s10311-021-01273-0
13. Tian, Zhi. "The effect of methanol production and application in internal combustion engines on emissions in the context of carbon neutrality: A review." Fuel 320 (2022): 123902. Doi: 10.1016/j.fuel.2022.123902
14. Zhen, X., & Wang, Y. (2015). An overview of methanol as an internal combustion engine fuel. In Renewable and Sustainable Energy Reviews (Vol. 52, pp. 477–493). Elsevier Ltd. Doi: 10.1016/j.rser.2015.07.083
15. Arapatsakos CI, Karkanis AN, Sparis PD. Behavior of a small four-stroke engine using as fuel methanolegasoline mixtures. SAE technical paper No. 2003-32-0024; 2003. Doi: 10.4271/2003-32-0024
16. Zhen XD. The engine knock analysis – an overview. ApplEnergy 2013; 112:431–9. Doi: 10.1016/j.apenergy.2011.11.079
17. Celik MB, Ozdalyan B, Alkan F. The use of pure methanol as fuel at high compression ratio in a single cylinder gasoline engine. Fuel 2011; 90:1591–8. Doi: 10.1016/j.fuel.2010.10.035
18. Vacca, A., Rossi, E., Cupo, F., Chiodi, M., Kulzer, A. C., Bargende, M., Villforth, J., Unger, T., & Deeg, H. P. (2022). Virtual Development of a Single-Cylinder Engine for High Efficiency by the Adoption of eFuels, Methanol, Pre-Chamber and Millerization. SAE Technical Papers. Doi: 10.4271/2022-37-0018
19. Dhaliwal B, Yi N, Checkel D. Emissions effects of alternative fuels in light-duty and heavy-duty vehicles. SAE technical paper No. 2000-01-0692; 2000. Doi: 10.4271/2000-01-0692
20. Anfilatov, A. A., & Chuvashev, A. N. (2020). Effect of methanol use in the engine on the workflow. IOP Conference Series: Materials Science and Engineering, 862(6). Doi: 10.1088/1757-899X/862/6/062064
21. Zembi J., Battistoni M., Mariani F. et al. Pressure and Flow Field Effects on Arc Channel Characteristics for a J-type Spark Plug. SAE Technical Papers 2022-01-0436. Doi: 10.4271/2022-01-0436

22. Zembi J., Mariani F., Grimaldi C., et al. Experimental and Numerical Investigation of the Flow Field Effect on Arc Stretching for a J-type Spark Plug. SAE Technical Papers 2021-24-0020. Doi: 10.4271/2021-24-0020
23. Abidin, Z. and Chadwell, C., "Parametric Study and Secondary Circuit Model Calibration Using Spark Calorimeter Testing," SAE Technical Paper 2015-01-0778, 2015, Doi:10.4271/2015-01-0778
24. Jung D, Iida N. An investigation of multiple spark discharge using multi-coil ignition system for improving thermal efficiency of lean SI engine operation. Appl. Energy 2018; 212:322–32. Doi: 10.1016/j.apenergy.2017.12.032
25. Jung D, Sasaki K, Iida N. Effects of increased spark discharge energy and enhanced in-cylinder turbulence level on lean limits and cycle-to-cycle variations of combustion for SI engine operation. Appl Energy 2017;205(August):1467–77. Doi: 10.1016/j.apenergy.2017.08.043
26. Breden, D.; Karpatne, A.; Suzuki, K.; Raja, L. High-Fidelity Numerical Modeling of Spark Plug Erosion. SAE Tech. Pap. Ser. 2019, 1, 1–12, Doi:10.4271/2019-01-0215
27. Wyczalek, F.A., Frank, D.L., and Nueman, J.G., "Plasma Jet Ignition of Lean Mixtures," SAE Technical Paper 750349, 1975, Doi:10.4271/750349
28. Toulson, E., Schock, H.J., and Attard, W.P., "A Review of Pre-Chamber Initiated Jet Ignition Combustion Systems," SAE Technical Paper 2010-01-2263, 2010, Doi:10.4271/2010-01- 2263
29. Mehdi, Ghazanfar, Sara Bonuso, and Maria Grazia De Giorgi. "Plasma assisted Re-ignition of aeroengines under high altitude conditions." Aerospace 9.2 (2022): 66. Doi: 10.3390/aerospace9020066
30. Starikovskiy, A. and Aleksandrov, N., "Plasma-Assisted Ignition and Combustion," Progress in Energy and Combustion Science 39, no. 1 (2013): 61-110, Doi:10.1016/j. pecs.2012.05.003
31. Singleton, D, Pendleton, S, Gundersen, M. The role of non-thermal transient plasma for enhanced flame ignition in C2H4-air. J Phys D Appl Phys 2001; 44: 022001. Doi: 10.1088/0022-3727/44/2/022001
32. S. M. Starikovskaia. "Plasma assisted ignition and combustion. " J Phys D Appl Phys 2006;39 (16):R265–99. Doi: 10.1088/0022-3727/39/16/r01
33. J. Zembi, et al. "Modeling of thermal and kinetic processes in non-equilibrium plasma ignition applied to a lean combustion engine." Applied Thermal Engineering, 2021, 197, 117377. Doi: 10.1016/j.applthermaleng.2021.117377
34. Starikovskii A. Plasma supported combustion. Proc Combust Inst 2005;30(2): 2405–17. Doi: 10.1016/j.proci.2004.08.272
35. Breden, D., Idicheria, C. A., Keum, S., Najt, P. M., & Raja, L. L. (2019). Modeling of a Dielectric-Barrier Discharge-Based Cold Plasma Combustion Ignition System. IEEE Transactions on Plasma Science, 47(1), 410–418. Doi: 10.1109/TPS.2018.2882830
36. Idicheria, C. A., Yun, H., & Najt, P. M. (n.d.). 1.3 An Advanced Ignition System for High Efficiency Engines. 40–54. Doi: 10.5445/IR/1000088317
37. Cruccolini, V., Discepoli, G., Ricci, F., Petrucci, L., Grimaldi, C., Papi, S., & Dal Re, M. (2020). Comparative Analysis between a Barrier Discharge Igniter and a Streamer-Type Radio-Frequency Corona Igniter in an Optically Accessible Engine in Lean Operating Conditions. SAE Technical Papers, 202-01-0276. Doi: 10.4271/2020-01-0276
38. Martinelli R., Ricci F., et.al, Lean Combustion Analysis of a Plasma-Assisted Ignition System in a Single Cylinder Engine fueled with E85, SAE Technical Papers, 2022-24-0034. Doi: 10.4271/2022-24-0034
39. Starikovskaia, S. M. (2014). Plasma-assisted ignition and combustion: Nanosecond discharges and development of kinetic mechanisms. Journal of Physics D: Applied Physics, 47(35). Doi: 10.1088/0022-3727/47/35/353001
40. Starikovskaia, S. M. (2006). Plasma assisted ignition and combustion. Journal of Physics D: Applied Physics, 39(16). Doi: 10.1088/0022-3727/39/16/R01
41. Irimescu, A., Tornatore, C., Marchitto, L., and Merola, S.S., "Compression Ratio and Blow-by Rates Estimation Based on Motored Pressure Trace Analysis for an Optical Spark Ignition Engine," Appl. Therm. Eng. 61(2):101-109, 2013, Doi: 10.1016/j.applthermaleng.2013.07.036
42. Ricci, F., Discepoli, G., Cruccolini, V., Petrucci, L., Papi, S., di Giuseppe, A., & Grimaldi, C. N. (2021). Energy characterization of an innovative non-equilibrium plasma ignition system based on the dielectric barrier discharge via pressure-rise calorimetry. Energy Conversion and Management, 244(April), 114458. Doi: 10.1016/j.enconman.2021.114458
43. Discepoli, G., Cruccolini, V., Dal Re, M., Zembi, J., Battistoni, M., Mariani, F., & Grimaldi, C. N. (2018). Experimental assessment of spark and corona igniters energy release. Energy Procedia, 148, 1262-1269. Doi: 10.1016/j.egypro.2018.08.001
44. Ricci, F., Cruccolini, V., Discepoli, G., Petrucci, L., Grimaldi, C., & Papi, S. (2021). Luminosity and Thermal Energy Measurement and Comparison of a Dielectric Barrier Discharge in an Optical Pressure-Based Calorimeter at Engine Relevant Conditions. SAE Technical Paper Series, 1, 1–11. Doi: 10.4271/2021-01-0427
45. Zembi, J., Ricci, F., & Grimaldi, C. (2021). Numerical Simulation of the Early Flame Development Produced by a Barrier Discharge Igniter in an Optical Access Engine. SAE Technical Papers, 2021-24-0011. Doi: 10.4271/2021-24-0011.

 doi:10.20944/preprints202403.0226.v1

46. Ricci, F., Zembi, J., Battistoni, M., Grimaldi, C., Discepoli, G., & Petrucci, L. (2019). Experimental and Numerical Investigations of the Early Flame Development Produced by a Corona Igniter. SAE Technical Papers, 2019-24-0231. Doi: 10.4271/2019-24-0231
47. Discepoli, G., Cruccolini, V., Ricci, F., di Giuseppe, A., Papi, S., & Grimaldi, C. N. (2020). Experimental characterization of the thermal energy released by a Radio-Frequency Corona Igniter in nitrogen and air. Applied Energy, 263(February), 114617. Doi: 10.1016/j.apenergy.2020.114617
48. Petrucci, Luca. "A Development of a New Image Analysis Technique for Detecting the Flame Front Evolution in Spark Ignition Engine under Lean Condition." Vehicles 4.1 (2022): 145-166. Doi: 10.3390/vehicles4010010
49. Ricci, F., Martinelli, R., Petrucci, L., Discepoli, G., Nazareno, C., & Papi, S. (n.d.). Streamers Variability Investigation of a Radio- Frequency Corona Discharge in an Optical Access Engine at Different Speeds and Loads. Doi: E3S Web of Conferences. Doi: 10.1051/e3sconf/202131207021
50. Cruccolini, V., Discepoli, G., Ricci, F., Grimaldi, C. N., & di Giuseppe, A. (2020). Optical and Energetic Investigation of an Advanced Corona Ignition System in a Pressure-Based Calorimeter. E3S Web of Conferences, 197. Doi: 10.1051/e3sconf/202019706019
51. Cruccolini, V., Grimaldi, C. N., Discepoli, G., Ricci, F., Petrucci, L., & Papi, S. (2020). An optical method to characterize streamer variability and streamer-to-flame transition for radio-frequency corona discharges. Applied Sciences (Switzerland), 10(7), 1–20. Doi: 10.3390/app10072275
52. Cimarello, A.; Grimaldi, C.N.; Mariani, F.; Battistoni, M.; Dal Re, M. Analysis of RF Corona Ignition in Lean Operating Conditions Using an Optical Access Engine. SAE Tech. Pap. 2017, 2017-01-0673, Doi:10.4271/2017- 01-0673
53. Germane, Geoff J., Carl G. Wood, and Clay C. Hess. Lean combustion in spark-ignited internal combustion engines-a review. Vol. 31. October, 1983. Doi: 10.4271/831694
54. Wu, Bin. "Comparison of lean burn characteristics of an SI engine fueled with methanol and gasoline under idle condition." Applied Thermal Engineering 95 (2016): 264-270. Doi: 10.1016/j.applthermaleng.2015.11.029
55. Eliasson, B.; Kogelschatz, U. Nonequilibrium volume plasma chemical processing. IEEE Trans. Plasma Sci.1991, 19, 1063–1077, Doi:10.1109/27.125031
56. Masurier, J-B.. "Ozone applied to the homogeneous charge compression ignition engine to control alcohol fuels combustion." Applied Energy 160 (2015): 566-580. Doi: 10.1016/j.apenergy.2015.08.004